Petrology and Geothermometry of Garnet Amphibolite Blocks, Santa Catalina Island, CA

A Senior Thesis presented to
The Faculty of the Department of Geology

Bachelor of Arts

Abigail Seymour
The Colorado College
May 2013

ABSTRACT

In the Santa Catalina Island, CA subduction complex, there are garnetiferous mafic gneiss blocks, from a tholeiitic protolith, that occur in a serpentinite mélange, a unit that is poorly understood and has been little studied in the last twenty-five years. Study of the microstructural relationships and geothermometry of two hand samples of garnet-rich gneiss yield information about processes and conditions for high temperature metamorphism in the Catalina complex and possibly more broadly. Results of the study provide insight into 1) the nature of HT metamorphism in the subduction setting, and 2) the metamorphic history of disparate gneiss blocks within the Catalina serpentinite mélange. Thin section petrography and scanning electron microscope (SEM) analysis were performed on polished thin sections of samples to identify minerals and microstructures. Compositional maps of garnets and quantitative mineral analysis of garnet, garnet inclusions, and matrix phases were acquired using an electron microprobe (EMP). The Zr-in-rutile geothermometer (Watson et al., 2006) was used to calculate peak metamorphic temperatures based upon Zr concentrations (ppm) for rutile inclusions and matrix measured by EMP. One of the garnet gneisses exhibits compositional zoning with Mg increase / Ca decrease toward the rim, and by a pattern of distribution of inclusions. The other sample has unzoned, compositionally homogeneous garnet with an unusual abundance of rutile for a metabasalt. The excess of rutile is a possible indication of metasomatism. Zr-in-rutile thermometry yielded temperatures of 480 to 516 °C for the study samples, in contrast to the results of Zack et al. (2004) of 764

to 800 °C for clinopyroxene-bearing garnet amphibolite in mélange blocks. The differing Zr-in-rutile results provide a possible indication that blocks in the mélange originated at vastly different depths in the subduction zone, then were brought together during mélange formation. My findings indicate that the two gneiss blocks studied have distinct protoliths and metamorphic histories, suggesting that mélange blocks within the upper tectonic unit of Catalina Island derived from different locations within a subduction zone.

INTRODUCTION

Santa Catalina Island, CA has a subduction complex that differs from typical subduction complexes in that there are amphibolite grade gneisses, produced by high temperature metamorphism, in the subduction mélange. Questions exist about the origin of the high temperature rocks in a subduction zone, when such zones normally are characterized by high pressure-low temperature assemblages. Temperatures in subduction zones are usually not hot enough to produce amphibolite metamorphism due to cooling from the cold subducting slab. The thermobarometry of the tectonic mélange, consisting of garnetiferous mafic gneiss blocks within a matrix of metasedimentary and metaultramafic rock, has been little studied in the last twenty-five years. Individual blocks may contain evidence of the metamorphic conditions in disparate parts of the subduction zone.

My research examines the petrography, garnet characteristics, mineral compositions, and accessory phases of two mafic gneiss blocks affected by high

temperature metamorphism. Each contains information about physical and chemical conditions that existed during subduction. Objectives are to gain insight into 1) the nature of HT metamorphism in the subduction setting, and 2) the metamorphic history of disparate blocks within the Catalina serpentinite mélange. The answers to these questions will shed light on the processes and conditions for high temperature metamorphism with subduction systems that are poorly understood.

GEOLOGIC BACKGROUND

Santa Catalina Island is located on the subduction margin of California. The rocks on the island are part of the subduction complex from this subduction zone. From structurally highest to lowest, the metamorphic assemblages include amphibolite, greenschist, and blueschist. This paper will focus on the garnet amphibolite blocks that are part of the amphibolite of the uppermost unit. Before diving into the specifics, we will first zoom out for an overview of similar packages of rock to understand some models in other locations.

Garnet-bearing ultramafic rocks occur predominantly in high-pressure and ultrahigh-pressure terranes in continent-continent collision zones, but are also rarely found in metamorphic belts related to subduction, such as in the Sanbagawa belt, Japan. The Sanbagawa belt consists of oceanic meta-sedimentary and meta-volcanic rocks that experienced metamorphism related to Cretaceous subduction. Their P-T path is a kinked, concave upwards, prograde path due to early, low P-T

conditions followed by a steep P/T gradient of prograde metamorphism. This path suggests either mechanical coupling with the subducting slab that dragged hydrated mantle down parallel to the slab-wedge interface, or ocean floor metamorphism and/or serpentinization during early stage subduction of ocean lithosphere followed by HP-UHP prograde metamorphism (Enami et al., 2004).

Garnet amphibolites make up some of the metamorphic subduction complex in central Palawan, Philippines. These garnet amphibolites have peak temperatures of 700-760 °C and minimum pressures of 9 kbar. The garnet grains show strong prograde zoning and contain inclusions that constrain pressures above 5-6 kbar at 400-500 °C, representing an early prograde clockwise path consistent with underthrusting. Peak metamorphic conditions in the earliest Oligocene was followed by rapid cooling and exhumation of the metamorphic rocks, perhaps due to the rapid thickening of the accretionary complex. It is interpreted that the amphibolites formed during the initiation of southward subduction within proto-South China Sea oceanic lithosphere (Encarnación et al., 1995).

Garnet and amphibole in eclogite blocks in the Northern Serpentinite Mélange of Cuba show oscillatory zoning that developed before peak conditions were attained. They indicate subtle fluctuations in P-T during prograde subduction and suggest episodes of retrogression-affected parts of the subducting slab (García-Casco et al., 2002).

In British Columbia, the Coast Plutonic Complex formed in response to crustal thickening due to the accretion of the Alexander and Wrangellia terranes to the Stikine terrane creating thrust slabs that were accompanied by intrusion of a

high-pressure pluton and associated sills. Pluton emplacement accompanied eastward directed thrusting of high temperature gneisses over low-grade rocks, inverting the metamorphic sequence (Crawford et al., 1987).

Baldwin and Harrison (1992) looked at the P-T history of blocks in serpentinite-matrix mélange in East San Benito Island and Cedros Island, west-central Baja California. Epidote-amphibolite and amphibolite facies blocks were metamorphosed during initiation of subduction in Mid-Jurassic, while coarse-grained blueschist blocks were metamorphosed during continued subduction in late Early Cretaceous time, showing the spatial association of blocks of at least two different ages. Blocks also underwent significantly different post metamorphic cooling histories indicated by fission track analyses of apatite (Baldwin and Harrison, 1992). In addition to the large age variations and contrasting cooling histories, blocks experienced different P-T-t paths. Thus, it is known that subduction related serpentinite matrix mélanges can contain blocks with diverse geological histories over relatively small length scales (<<1 km).

The Catalina Schist is considered to be correlative to the Franciscan Subduction Complex of the California margin (Rowland, 1984). The Franciscan Complex and the Catalina Schist have very similar characteristics, including the presence of amphibolite blocks within serpentinite matrix mélange in the structurally highest zone, with mineral assemblages indicative of basaltic or gabbroic protoliths (Wakabayashi, 1990). The amphibolite blocks of the Franciscan record a counter clockwise P-T-t path that is explained by Wakabayashi (1990) in a tectonic model involving the basalt of the subducting plate metamorphosed in

amphibolite facies by the heat of the overriding plate. The amphibolite was scraped off and accreted to the upper plate, keeping it at depth as it equilibrated, then cooled.

The blueschist unit of the Catalina Schist contains protoliths with ages that overlap the oldest part of the Pelona-Orocopia-Rand schists. The Pelona-Oracopia-Rand schists are similar to the Franciscan Complex but are structurally located beneath the Cretaceous marginal arc batholith instead of being outboard of the forarc basin. Jacobson et al. (2011) propose that the Pelona-Orocopia-Rand schists and the Catalina Schists were connected to the initiation of the Nacimiento fault. They suggest that after the Farallon plate commenced shallow subduction, potentially due to a presence of an aseismic ridge or oceanic plateau, the conditions favoured underplating of the schists (Fig. 1B). The Nacimiento fault interrupted the continuity of the units and accommodated either thrust or strike-slip motion (Jacobsen et al. 2011). Thus, there are inboard rocks that provide information about the margin processes.

On Catalina Island, CA, there are three main tectonic units with different metamorphic mineral assemblages on Catalina Island, CA (Fig. 2). The blueschist unit is structurally lowest and consists of metagraywacke, metachert, mafic metavolcanic rocks, and ultramafic rocks. Most of the volcanic rock is interstratified basaltic sandstone and conglomerate that has been recrystallized to glaucophane-lawsonite schist and phyllites (Platt, 1975).

The greenschist unit structurally overlies the blueschist unit and contains some of the same rock types but with a higher proportion of metamorphosed mafic

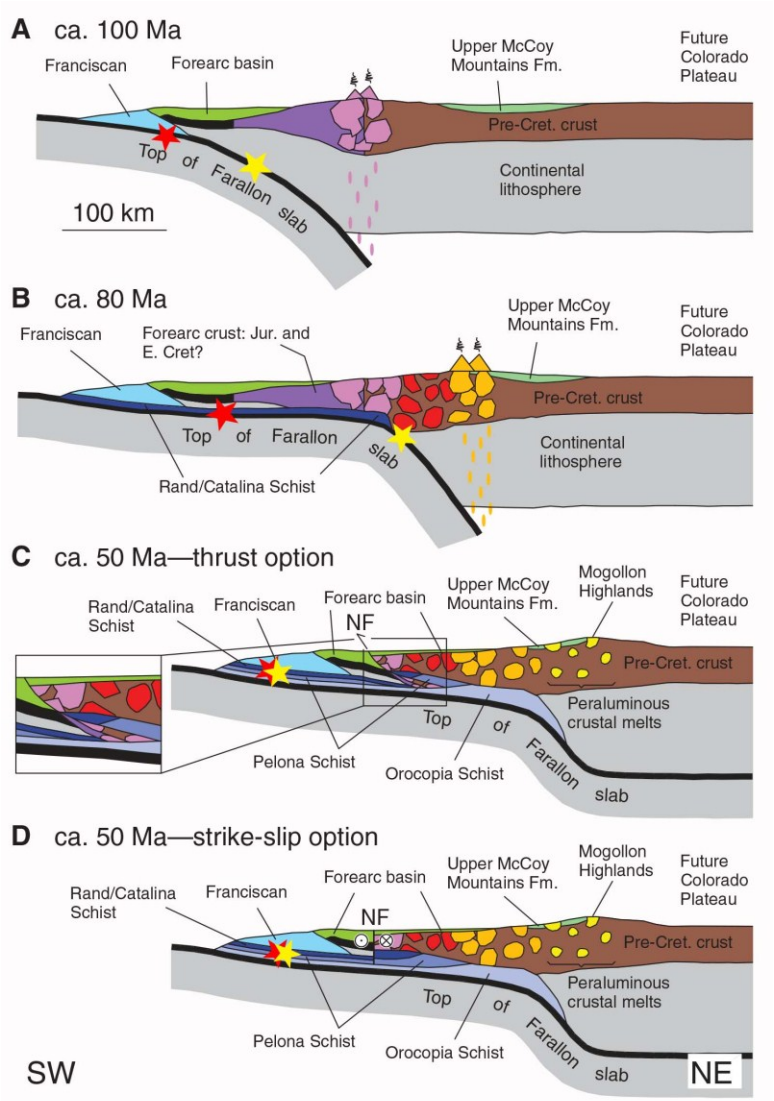

Figure 1. Tectonic model (Jacobson et al, 2011) for underplating of the Pelona-Orocopia-Rand schists and Catalina Schist and the development of the Nacimiento fault. A) Geometry prior to the onset of flat subduction and emplacement of schists. B) Early phase of flat subduction. C-D) Relations following cessation of slope along the Nacimiento fault, modelling thrusting and sinistral strike-slip respectively. Figures 3C and 3D show scenarios for thrusting and strike slip for the Nacimiento fault respectively since the type of fault is unknown. One scenario shows thrusting of the Nacimiento fault with material being interleaved in with the schists (Fig. 3C). The alternative is a strike-slip model of the Nacimiento fault with the excess material being moved away laterally (Fig. 3C). The stars indicate depths for blocks; red is blocks with T's ~500 °C and yellow is blocks with T's ~700 – 800 °C. Stars in A and B indicate starting depths of blocks depending on the time and therefore slope angle of the slab. Stars in C and D show that by this time the blocks have to have been moved west in order to be on the side of the fault which they end up on, at Catalina Island.

volcanics and metapelite. There are obvious porphyroblasts of clinozoisite and epidote in the mafic schist and in the metasediments of albite, almandine garnet and locally biotite (Platt, 1975).

The amphibolite unit is the uppermost unit on the island. It is predominantly made up of green hornblende-zoisite schist with a body of massive serpentinite on top. Isolated garnet amphibolite blocks occur within the serpentinite. The green hornblende-zoisite schist has an igneous protolith (Platt, 1975).

The three tectonic units are fault-bounded, so primary contact relationships are not preserved (Fig. 3). The contact between the blueschist and the greenschist is subhorizontal with the greenschist Unit on top. The fault boundary, called the Greenschist-Blueschist thrust, is a zone up to 200 m thick. The zone is a mélange containing tectonic blocks of amphibolite facies gneiss and serpentinite (Platt, 1975). The Ollas Thrust is the contact between the amphibolite and underlying greenschist. The thrust is subhorizontal with a very shallow north to northeasterly dip. It is postmetamorphic and crosscuts the Greenschist-Blueschist thrust (Platt, 1975).

The Catalina tectonic package has an inverted temperature (T) gradient, in that the rocks affected by higher metamorphic temperatures overlying rocks metamorphosed at lower temperatures. This is counter to the expectation for the typical crustal condition where temperature increases with depth. The temperature field gradient decreases downward and westward from the subduction boundary (Platt, 1975), with the highest-grade rocks on top of lower grade rocks. There is also

an age inversion, with upper highest-grade rocks determined to be circa 115 Ma, and lower rocks circa 97-95 Ma (Grove et al., 2008).

Several hypotheses have been developed in an effort to explain the presence of the amphibolite gneisses and the T and age inversions. Platt (1975) hypothesised that there was an onset of subduction at 115 Ma, with transfer of a slice of oceanic crust that became the amphibolite gneiss unit to the base of the overriding plate and a halt to its downward motion. The scheme resembles that of Wakabayashi (1990). The subduction continued upon a tectonic boundary beneath and under the mafic package that became part of the Catalina subduction complex. The hanging wall of the subduction zone would have been initially hot enough, about 710 °C at 10 kbar, to metamorphose the sliver of oceanic crust at amphibolite conditions. High-grade rocks were emplaced onto lower-grade rocks by a reverse fault dipping eastward caused by the force of plate convergence. The metamorphic complex then cooled and was uplifted (Platt, 1975).

An alternative hypothesis from Grove and Bebout (1995) is that an oceanward step out of the subduction zone was caused by the suturing of an island arc complex onto the western edge of North America, resulting in a new subduction zone at ~120-115 Ma. The Catalina subduction complex was formed from the underplating of oceanic crust within this newly initiated subduction zone. An alternative hypothesis (Grove et al. 2008) is that the Catalina subduction complex was underthrust beneath the western Peninsular Ranges batholith, which supplied magmatic heat for metamorphism and formation of the inverted T gradient in subducted oceanic crust. Then, subduction erosion caused the juxtaposition of the

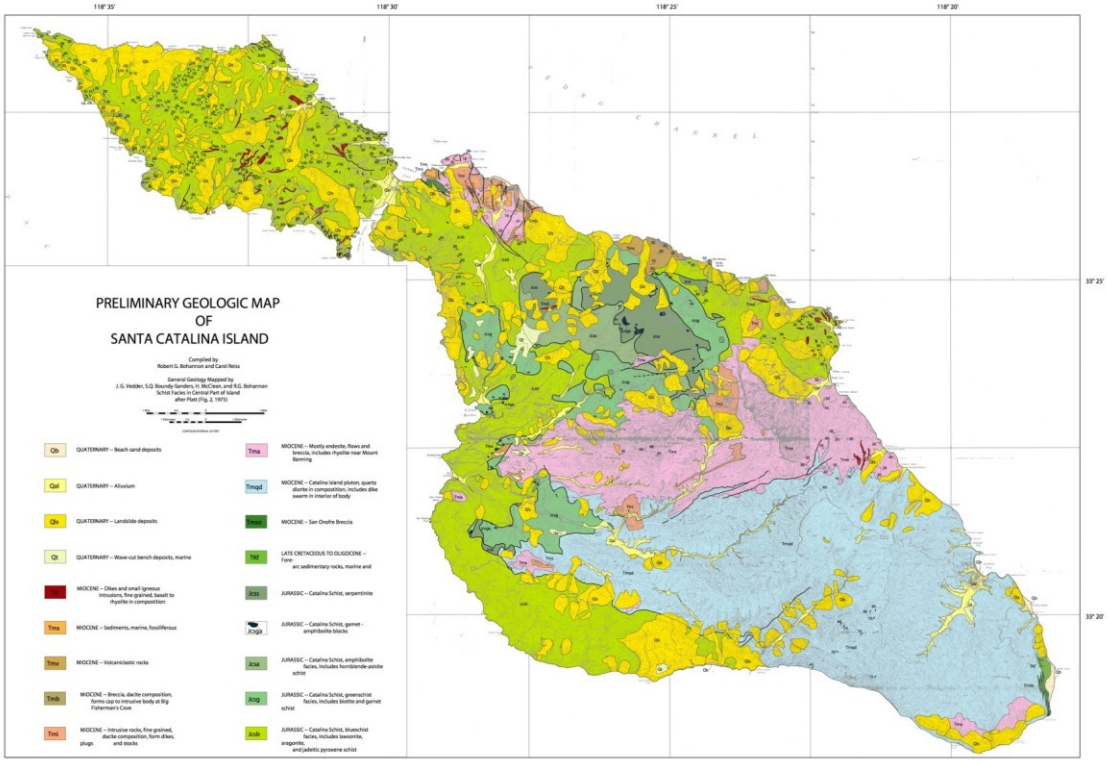

Figure 2. Geologic map of Catalina Island. Dark greens are amphibolite unit, bright intermediate green is greenschist unit, and lime green is blueschist unit. Pink is Miocene volcanic rock mostly andesite, light blue is Miocene quartz diorite pluton, oranges are Miocene volcaniclastic and dacite breccias, and yellows are Quaternary sedimentary deposits (Bohannon and Reiss 1998, based off of Platt 1975).

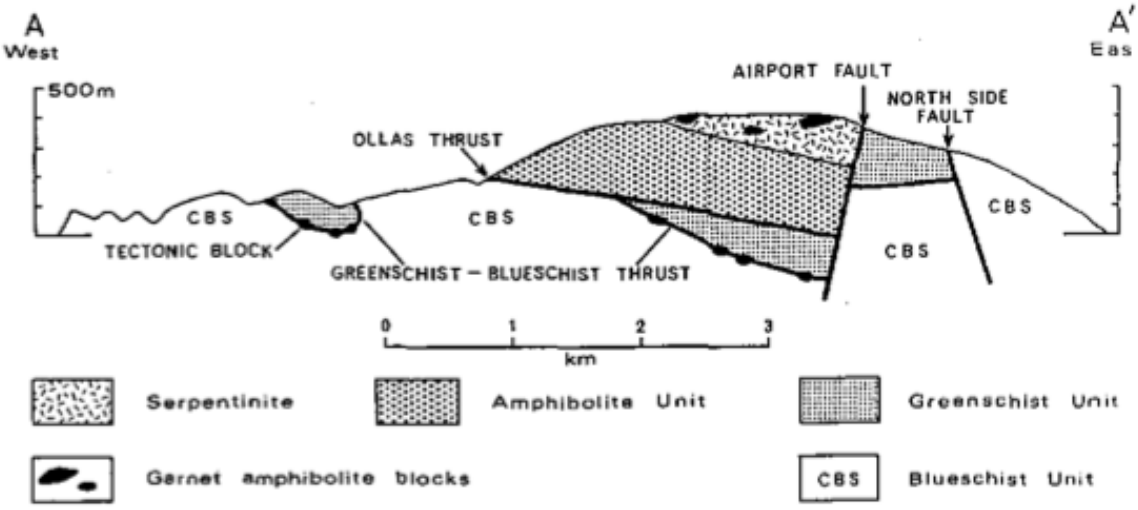

Figure 3. Cross-section of Catalina Island showing the relationship of the units. Amphibolite unit is at the top, overlying the greenschist unit, and then the blueschist units, all separated by faults (Platt, 1975). Garnet-amphibolite blocks are depicted as black blobs within a serpentinite matrix, at approximately the elevation and location that is shown. Amphibolite lenses also occur along the Greenschist-Blueschist thrust.

amphibolite package with low-pressure rocks (Grove et al., 2008).

In 2004, Zack et al. used the new Zr-in-rutile thermometry technique to determine the temperature of formation of rocks in several different locations, including garnet amphibolites from Catalina Island. His analysis of three garnet amphibolite blocks resulted in temperature of 764 to 800 °C. This is the most recent analysis of the temperature of metamorphism for the amphibolite unit.

The matrix for the amphibolite unit is made up of serpentinite that has low-T mineral assemblages and hornblende-zoisite schist with Si-rich, hydrous high-T assemblages. The process of serpentinization entails hydration of ultramafic mineral phases. Serpentinization postdated and was lower temperatures than other metasomatism experienced throughout the package (Sorensen & Grossman, 1989). The amphibolite assemblage is cut by pegmatite leucocratic dikes (Sorensen & Grossman, 1989) that are thought to have trondhjemitic compositions as result of hydrous melting process (Sorensen, 1988). The protoliths for the matrix of hornblende-zoisite schist and serpentinite is harzburgite and dunite (Platt, 1975), whereas the garnet gneiss blocks are thought to have derived from a tholeiitic protolith (Sorensen and Barton, 1987). Thus, the mineral makeup, petrogenesis, and geochemistry of the garnet gneiss blocks differ between blocks and contrasts starkly with the surrounding serpentinite matrix.

The three types of garnet amphibolite blocks are 1) non-migmatitic, clinopyroxene-bearing gneiss; 2) gneiss with alteration rinds, or blackwall; and 3) gneiss containing leucocratic segregations, described as migmatitic. The geochemistry of the non-migmatitic, clinopyroxene-bearing blocks resembles mid-

ocean ridge basalt (MORB) depleted of an albite component (Sorensen and Grossman, 1989). The rinds suggest local chemical interaction between the block, matrix and a fluid. The migmatitic gneisses are enriched in trace elements including High Field Strength Elements (HFSEs) and Rare Earth Elements (REEs), as a result of infiltration by aqueous fluid, which in turn could have introduced Na-Al silicate (Sorensen, 1988, and Sorensen and Grossman, 1989). This aqueous fluid in a complex metasomatic and metamorphic series is thought to have caused partial melting at relatively low pressure for melting, P = ~8.5-11 kbar and T = ~640 to 750 °C (Sorensen and Grossman, 1989).

Thermobarometry is the determination of the temperature and pressure at which metamorphic, or igneous, rocks formed and reached chemical equilibrium, using quantitative methods. This is important because having knowledge of the P and T at equilibration allows for determination of where and how the rock formed. Classical thermobarometry uses assemblages of coexisting minerals in equilibrium that form by reactions that are sensitive to either temperature (for a thermometer) or pressure (for a barometer), but does not depend significantly on the other (Whitney, 2013). Pairs of minerals are analysed using an electron microprobe (EMP) to obtain compositions. This compositional data along with enthalpy, entropy, volume, and heat capacity of reaction data that is known and documented is used to graph a line of constant equilibrium on a P-T diagram. Interpretation is that the rock must have equilibrated along the line, since both minerals are present in equilibrium in the sample (Spear, 1993). A more general application of the

approach uses petrogenetic grid constraints to determine the P-T field for metamorphism.

Equilibrium modelling on the other hand uses compositional data from XRF analysis to calculate a P-T pseudosection. Using this method, thermobarometric information is obtained from the position in P-T space of the mineral assemblage and the proportions and compositions of the minerals that are contained in the area. This method assumes that the rock is homogenous on the appropriate scale and that the mineral assemblage is in equilibrium. In conjunction with this, it also assumes that the rock is a closed system, without fluids or anything else coming in and altering it from the outside (Powell and Holland, 2008). Conventional thermobarometry and mineral equilibrium modelling are unsuitable methods for the Catalina amphibolite blocks because disequilibrium evidence exists throughout the study samples at the scale of the thin section. However, an alternative new method offers a means to determine temperature of metamorphism.

Zr-in-rutile thermometry is new accessory phase geothermometry technique that has only been in use since 2004 (Zack et al., 2004). By putting the concentration (ppm) of Zirconium in a rutile grain into a calibration equation, the temperature at which the rutile crystal grew can be calculated. This method is thought to be valid because it is believed that Zr concentrations are homogenous in rutile grains independent of size, similar temperatures result from similar textural settings, and diffusion of Zr is not likely to have affected its distribution after the formation of the rutile grain (Spear et al., 2006).

STUDY AREA

Fieldwork was done as part of a Keck Geology Consortium project on Santa Catalina Island, California, from July 4-20, 2012. The island lies off the coast of California, south of Los Angeles. It is 35.4 km long by 13 km across with a high point in the middle, Mount Orizaba, where the airport is located. It has a mild subtropical climate. It is dry in the inland part of the island with many cacti, especially prickly pear and shrubby brush. There are many drainages that arise upon Mount Orizaba and widen towards the ocean with ridges in between (Fig. 4). The valleys are occupied by beaches at the coast, whereas the ridges terminate in cliffs or bouldery shoreline.

My samples were collected from isolated garnet-amphibolite blocks within serpentinite on the northeastern quadrant of the island. Three samples are from a large block located at (33.41592° N, 118.44010° W) including sample H2718D. This block is about 4 m high by about 8 m wide. Surrounding vegetation conceals the serpentinite "matrix" rock (Fig. 5). Amphibolite facies gneisses form a hill behind the block, so this block could have fallen from higher up in the unit, or the surrounding serpentinite could have been eroded away leaving the block behind. We chose to sample this block for several reasons. One was the presence of large, prevalent garnets as well as what appeared to be plagioclase feldspar webbing through the block. There was also a large plagioclase and quartz vein that ran through the block. This indicated that this block could have experienced migmatization, something that

Figure 4. View to the North on Santa Catalina Island. (Photo by Zeb Page)

Figure 5. Large block of competent amphibolite. Softer weathering bed rock around it probably is serpentinite.

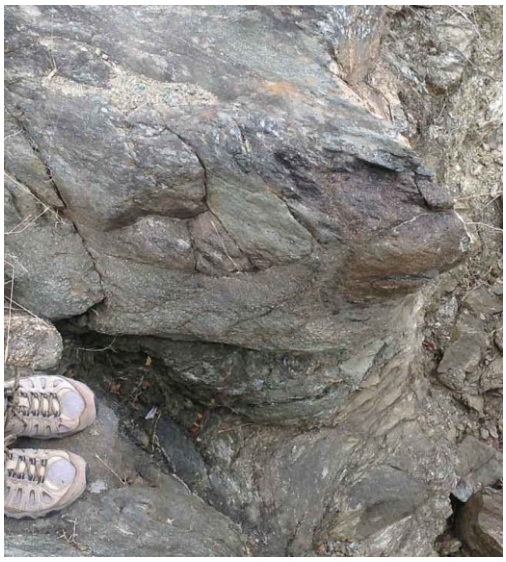

Figure 6. Competent garnet- garnet-amphibolite
block in situ surrounded by ultra mafic mélange in Valley of Ollas. (Photo by Zeb Page)

we were interested in exploring because it gives a window into what happened to the block during the subduction process.

Sample 712C-1 is from a foliated garnet amphibolite block that was in situ in the ultra mafic mélange (Fig. 6) at the top of the Valley of Ollas at (33°25.126096' N, 118°25.933292W). This block is exposed in the bottom of a bedrock channel at a small drop off, where erosion by the seasonal river exposed rock. This block was sampled because its assemblage is garnet and amphibole with visible foliation. Its original location is certain since it was in situ. It also allowed us to sample the corresponding serpentinite matrix.

ANALYTICAL METHODS

Methods used for research include band saw cutting, microscopy, carbon coating, scanning electron microscope and electron microprobe analysis, and temperature calibration. To prepare thin sections, samples were cut into slabs on a band saw during rock processing at Oberlin College, from July 22-30, 2012. Slabs were cut into billets, and the billets were used to prepare polished thin sections by the lab technician at Oberlin College in September and October 2012. The polished thin sections were sent to me at Colorado College.

Petrographic analysis was accomplished using a Leitz Laborlux 12 Pol S petrographic microscope for identification of minerals and microstructures. Photomicrographs were taken using a Canon EOS Rebel T4i and EOS Utility software. Thin sections were carbon coated with a Denton Vacum DV-502A.

The JEOL JSM-6390LV scanning electron microscope (SEM) at Colorado College was used to acquire qualitative elemental analyses of garnet inclusions. Utilizing a JEOL microprobe (EMP) at the University of Wyoming, compositional maps of garnets were made by technician Susan Swapp. The maps guided quantitative mineral analysis of garnet, garnet inclusion, and matrix phases that are used to evaluate P-T changes during garnet growth, also using the JEOL superprobe. Operating conditions of 200nA 15kV with beam diameter of 15um were used, following conventional mineral standardization using Gore Mountain and spessartine garnet, Kakanui amphibole, and albite standards. The composition zoning in the garnets and distribution of inclusions provides information about P-T evolution during growth of garnet. At Rensselaer Polytechnic Institute, Zr concentration (ppm) of rutile, in polished sections, was analysed by a Cameca SX 100 EMP standardized to rutile and zircon with operating conditions of 200 nA and 15 kV and a beam width of 0 um, assisted by technician Dan Ruscitto. The Zr-in-rutile geothermometer (Watson et al., 2006; Eq. 1) was used to calculate peak metamorphic temperatures for the two samples. The criteria for use of the thermometer are generally that quartz or baddeleyite coexist with the rutile, but if neither of these are present, the activity of ZrO_2 in zircon would be constrained between the limits of the other two but unbuffered but still possibly to use (Watson et al., 2006).

$$\mathrm{T}\ (^{\circ}\mathrm{C}) = \frac{4470}{7.36 - \log(\mathrm{Zr})} - 273 \qquad \text{Equation 1}$$

SAMPLE DESCRIPTIONS

Sample 712C-1

Sample 712C-1 is foliated garnet amphibole gneiss. It contains garnet, amphibole, and rutile. Garnet (estimated 30%) forms euhedral, inclusion rich porphyroblasts with diameters of 0.35-2.5 mm. The groundmass is euhedral amphibole (estimated 67%) that has a shape preferred orientation and uniform length of 0.75 mm (Fig. 7D). Rutile (estimated 3%) is throughout the groundmass as anhedral and euhedral grains (0.05-0.2 mm). Apatite and monazite appear as small, rounded accessory grains.

Garnets have two to four zones denoted by the distribution and abundance of inclusions (Fig. 7A-C). All garnet interiors are inclusion rich with numerous, small (~0.03 mm), sub-rounded inclusions. The outermost ~0.23 mm is inclusion free. There is no evident alignment of inclusions. Some garnets contain large ~0.2-0.25 mm round inclusions in their centers. In some garnets, a "ring" of elongated minerals that crystallized along a relict garnet border demarcates the inclusion-rich core and inclusion free rim.

Compositional maps created using the EMP show that garnet is compositionally zoned (Fig. 8A-D), with rims exhibiting increased Mg and decreased Ca compared to the interior garnet. Fe and Mn show no change throughout garnet.

Truncation of aligned amphiboles against garnet indicates that garnet growth post-dated solid-state deformation that formed foliation (Fig. 7F). Bordering garnet, amphibole exhibits undulose extinction and cracking (Fig. 7E). From microstructure

observation, the interpreted order of events is amphibole growth during tectonism with development of foliation under differential stress conditions. Subsequently, euhedral garnet formed. This is indicated by the lack of wrapping foliation around the garnets, which would form by an intensification of strain around the garnets.

Inclusions in garnet, which were too small to identify optically, were identified by SEM/EDS as albite and epidote, with some rutile. Rarely there is accessory titanite, quartz, and amphibole. The albite and epidote form symplectite. Inclusions in the intermediate zone are estimated as 70% quartz, 17% amphibole, and 13% rutile. Amphibole and rutile coexist with quartz in inclusions and also occur separately. The inclusion phases, or elongated rutile alone, mimic the shape of an old grain boundary (Fig. 7G). Albite is found only as inclusions, and then only as feldspar-epidote symplectite that is not present in the groundmass. There is no leucosome present.

A brittle structure, evident as a network of cracks with distinct evidence of alteration, possibly oxidation, cuts through the sample (Fig. 9). The cracks represent a possible fluid migration pathway.

Sample H2718D

Sample H2718D is garnet rutile gneiss lacking foliation. It contains garnet, amphibole, and rutile. Garnet (estimated 47%) porphyroblasts have a diameter of 0.5-3 mm and are sub- to anhedral. They form masses of coalesced grains (Fig. 10A). The groundmass is composed of amphibole (estimated 14%) and rutile (estimated

Figure 7. Sample 712C-1 A) An example of the garnets that contain two zones. The innermost zone contains small, isolated, sub-rounded inclusions. The outer zone is inclusion free. B) A garnet that presents three zones, with the innermost having three large inclusions; succeeded by an inclusion rich zone, then a zone that is inclusion free, C) A garnet with four zones discerned by the differences in inclusion distribution. This garnet shows a large inclusion in the core surrounded by a zone of small, sub-rounded inclusions. There is a thin zone of elongated minerals before the inclusion free border. D) Aligned amphibole that defines a dynamic fabric. E) Fractured amphiboles next to garnet record differential stress arising from impingement on the amphibole. F) Amphiboles truncated against garnet, with absence of wrapping foliation indicate that growth of garnet porphyroblasts occurred after amphibole formation and deformation. G) Rutile inclusions parallel to the garnet margin, suggesting that the precipitation of the plagioclase and amphibole was influenced by a relict garnet margin. (A-F are cross-polarized light, 5x magnification, G is plain polarized light, 10x mag.)

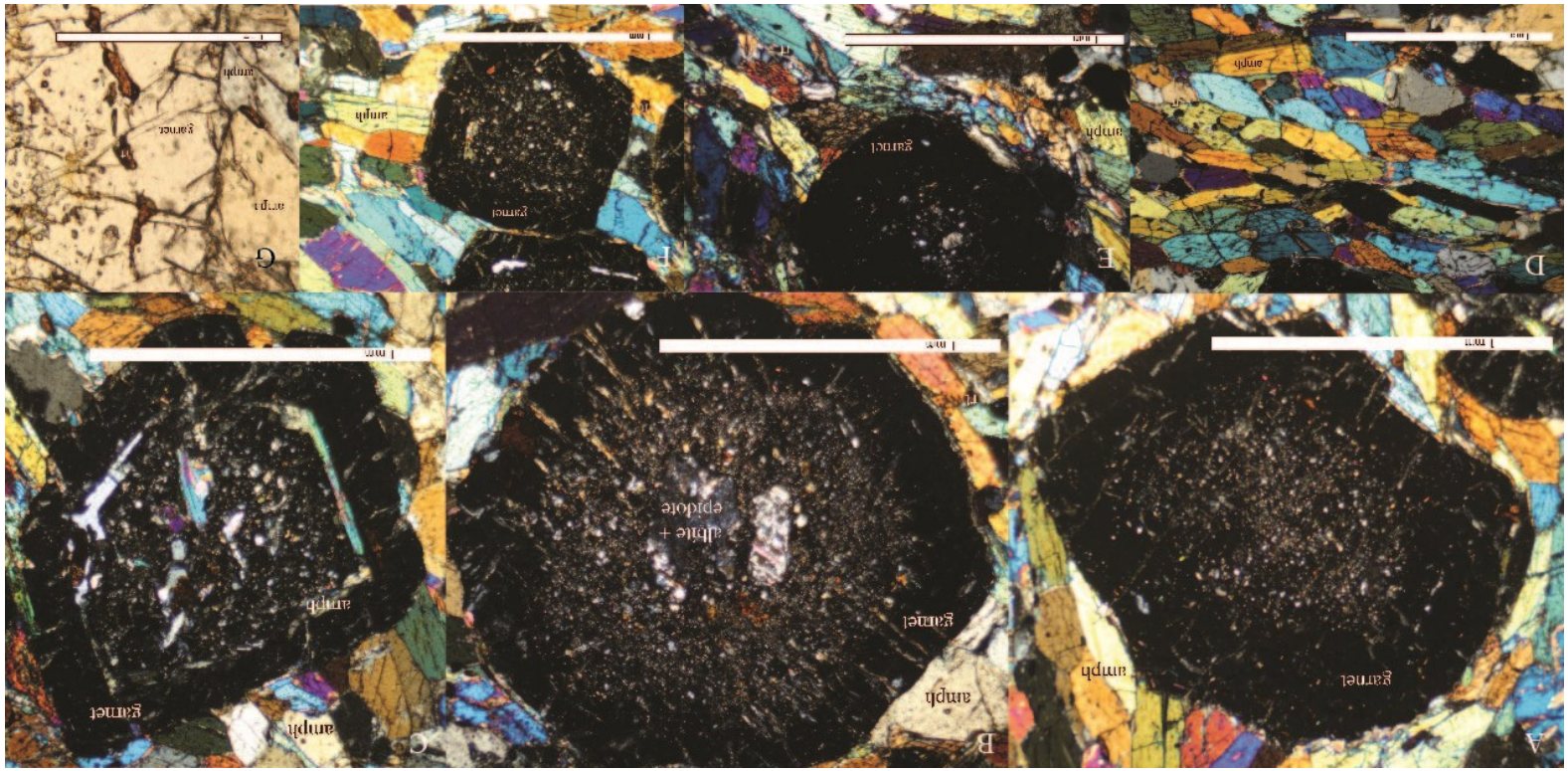

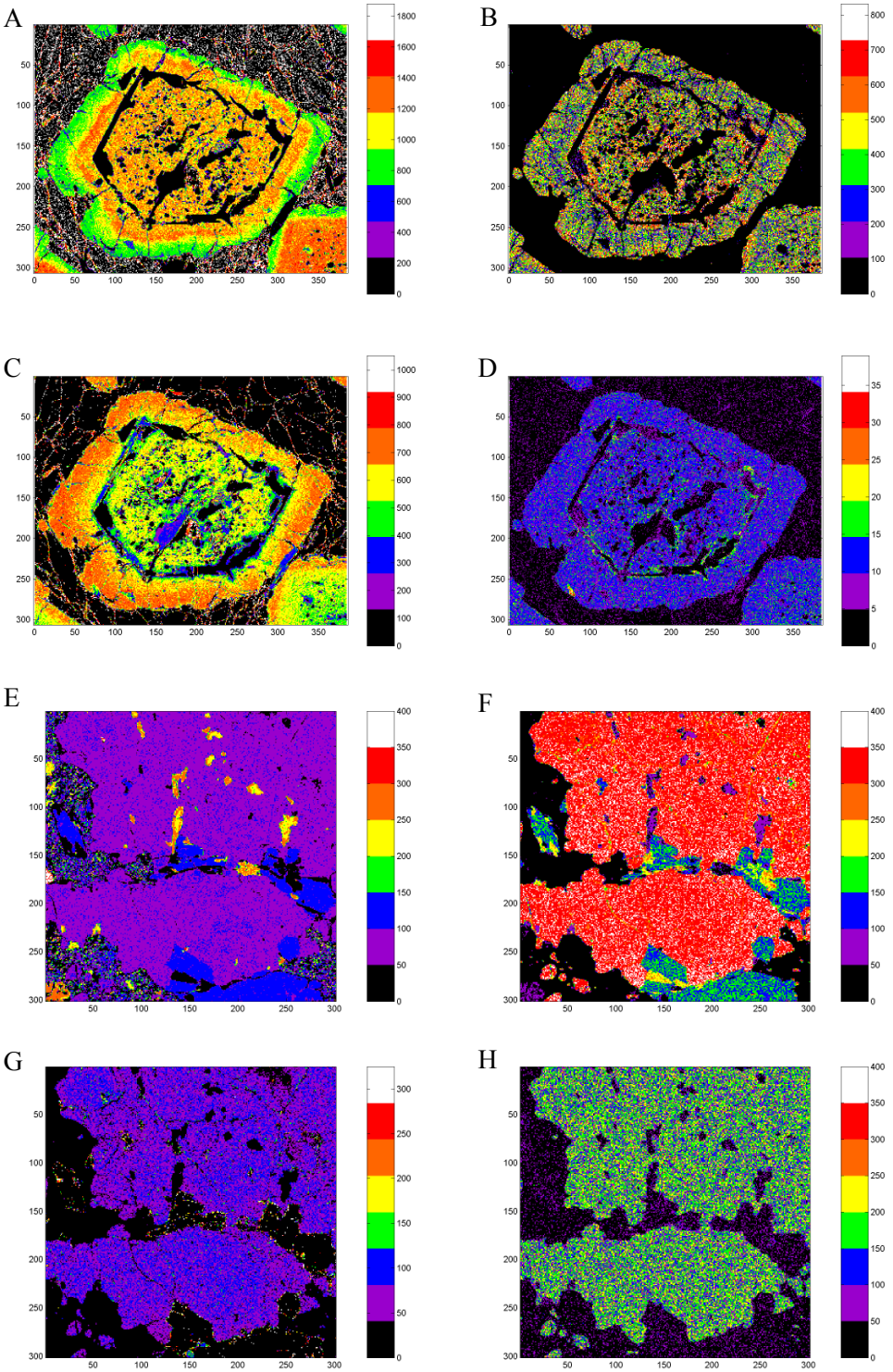

Figure 8. Compositional maps. A-D: garnet, sample 712C-1. E-H: garnet, sample H2718D. A) Ca map, showing depletion in the rim. B) Fe map, patchy and does not show zoning. C) Mg, enriched near the rim. D) Mn, patchy and unzoned. E) Ca. F) Fe. G) Mg. H) Mn. Distribution of elements for sample H2718D are patchy and do not indicate zoning.

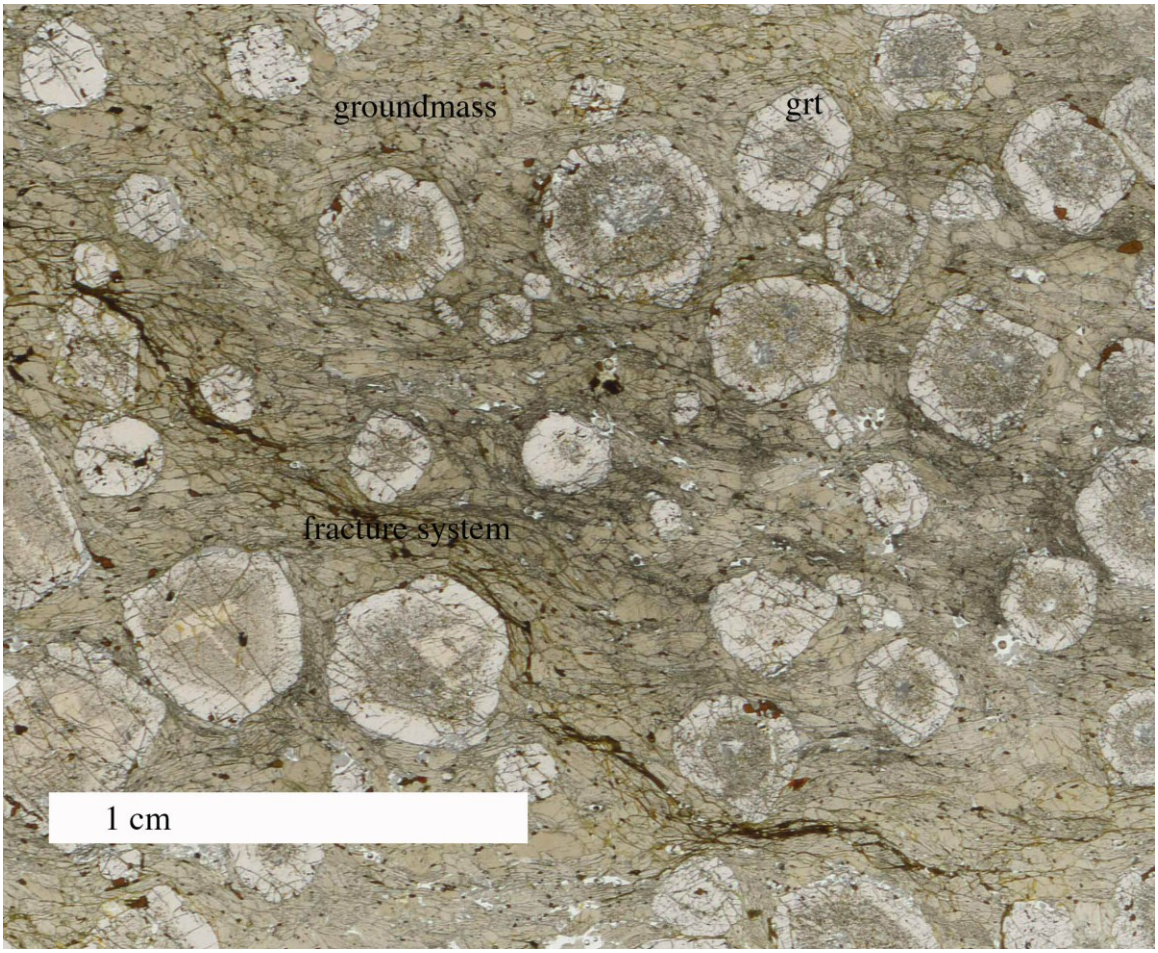

Figure 9. 712C-1 shows microcracks through the sample with focused alteration along fracture net. There is a decrease in the number of cracks towards the upper right and lower left of the image, progressing away from the most intense zone of fracturing. (Plain-polarized light)

18%). The amphiboles are sub-euhedral to anhedral, with lengths of 0.1-0.5 mm. Rutile forms large, anhedral grains (~0.05-1 mm wide) distributed around the perimeter of garnet (Fig. 10B) and as small grains in the groundmass. The large rutiles are rimmed by titanite (Fig. 10D), but the smaller rutiles ordinarily lack titanite rims. There is a significant amount of bluish grey alteration material (21%), which forms a web-like net throughout the groundmass, fingers along fractures, into some of the garnets, and corresponds to altered garnet cores. Accessory phases are

zircon, apatite, and monazite. Sparse chlorite appears as a retrograde mineral in association with rutile (Fig. 10C).

Garnets are coalesced garnets that show microstructures of impingement and moulding around each other. The garnets of sample H2718D are un-zoned. No changes of distribution or size of the sparse inclusions are discernable; the inclusions are all isolated and tiny. The distribution of inclusions does not indicate a relict garnet border. Spot SEM and EMP composition map analyses do not suggest compositional differences between garnet cores and rims.

Symplectic textures are found in several locations in the sample (Fig. 10E). Two are encircled by garnet and one is in the middle of groundmass amphiboles. This texture indicates disequilibrium.

Compositional maps of garnet were obtained using the EMP (Fig. 9E-H). The garnets show a lack of compositional zoning in Ca, Fe, Mg, and Mn, in addition to the lack of zoning indicated by the distribution of inclusions. This suggests that garnet in this sample is homogeneous and equilibrated. The garnet does not coexist with the other equilibrium minerals that are suitable for thermobarometry, however.

Mineral phases that were too small to distinguish optically were identified by SEM/EDS. The symplectite is composed of albite and epidote, and the symplectite relationships indicates breakdown of a pre-existing Ca-Fe phase that was in disequilibrium.

No quartz is present and albite is the only feldspar present, in disequilibrium textures. There is no leucosome present.

A brittle structure goes through this sample, indicated by a microgranular

Figure 10. Photomicrographs of sample H2718D. A) Clump of coalesced garnets, with minor amphibole or alteration material in between the garnet perimeters. B) Rutile is located around the perimeter of garnet. C) Chlorite (retrograde) and symplectite. D) High relief, transparent rim of titanite surrounding rutile is common on the large rutile grains. E) Albite and epidote symplectite, a disequilibrium microstructure. (All images are cross-polarized light, A + B are 5x magnification and C-E are 10x magnification.)

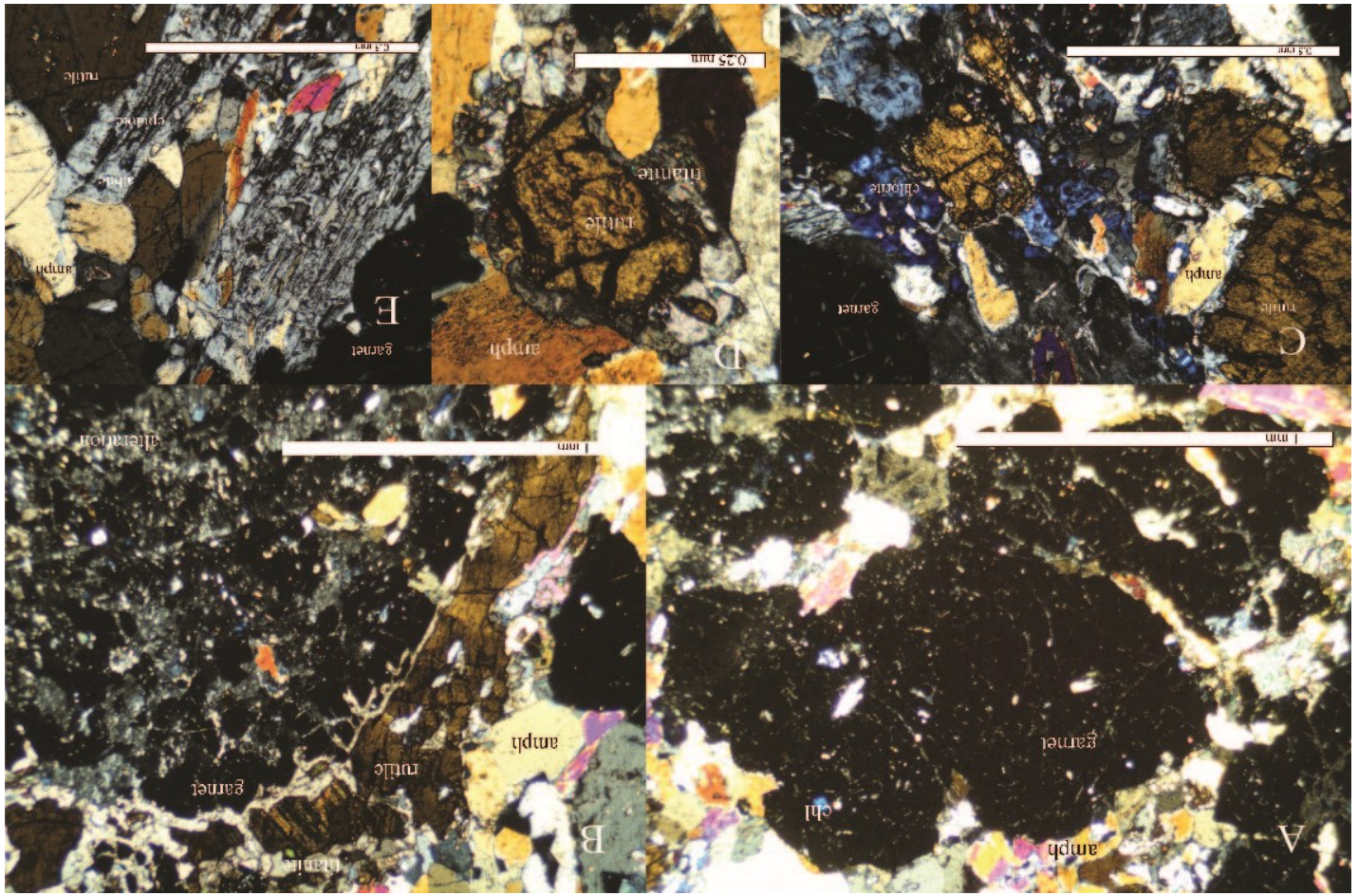

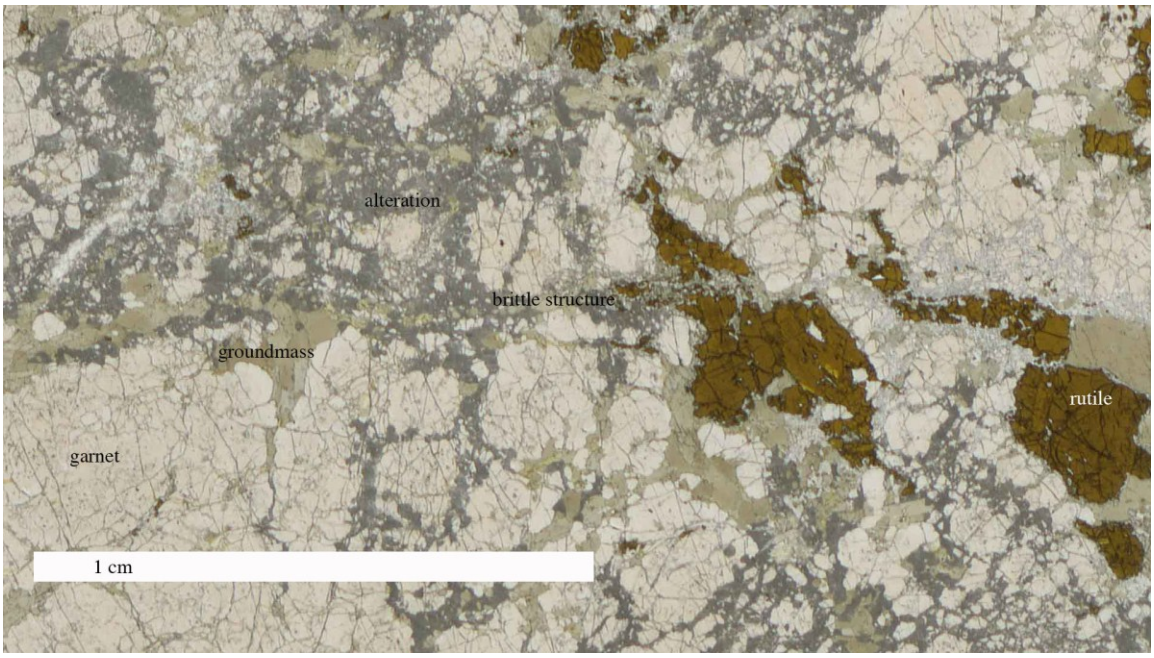

Figure 11. Fracture system in thin section H2718D, shown by broken up minerals and crosscutting of rutile runs horizontally across the middle of the image. Deformation is very localized in a zone about .4 mm thick. (Plain-polarized light)

texture (Fig. 11). It appears to crosscut the rutile and alteration material seems to run along it. This fracture system could have allowed fluid to flow through, altering the composition of the surrounding minerals.

RESULTS

Mineral Chemistry

Garnet

Garnet, amphibole, and plagioclase were analysed on the EMP. The garnet in samples 712C-1 and H2718D is almandine. Low totals on some analyses suggest a possibility that some zones are granditic (S. Swapp assessment, 2013).

Sample 712C-1 shows elemental zoning of major elements between the garnets core, intermediate, and rim. Between the core and intermediate zone, Fe and Al decrease, although between the intermediate zone and the rim the Al increases very slightly but Fe remains the same. Mg increases near the rim, with a decrease in Ca and Mn (Table 1, part 1).

Sample H2718D does not show variation in composition from core to rim, or between garnets located outside and within the brittle fracture. The core has lower Ca and the rim has lower Mn and Fe (Table 1, part 1). However, other than those slight differences the garnet is chemically homogeneous in respect to major elements.

Amphibole

The amphibole in sample 712C-1 changes from pargasite inclusions in the intermediate zone to gedrite in the relict border to tschermakitic in the groundmass. The major elements of amphibole inclusions do not smoothly increase or decrease from the interior of garnet to the outside; but rather vary in an irregular fashion. Within garnet, from the intermediate inclusions to the relict border inclusions Ti, Ca, and Na decrease and Mg, Fe, Mn, and Cl increase. But from the inclusions to the groundmass, Al decreases but Ti, Na, and K increase (Table 1 part 2).

According to its major element composition, the groundmass amphibole in sample H2718D is tschermakitic. In close proximity to garnet, the groundmass amphibole increases in Na (Table 1, part 2), but amphibole inclusions were not

Table 1. Representative mineral make-ups of garnet, amphibole, and feldspar

Garnet	[redacted]		712CE[redacted]			H2718D		[redacted]
	Core	Intermediate	Rim	Core	Intermediate	Rim		Brittle/Fx
SiO2	39.294	39.075	39.201	38.351	38.336		37.917	38.659
MgO	5.399	4.687	6.578	4.071	4.029		4.072	3.831
Na2O				*Not(Measured*				
Al2O3	21.113	21.258	21.629	21.003	20.987		20.908	21.082
FeO	30.347	29.028	28.186	27.321	26.948		25.443	27.289
MnO	0.933	1.155	0.83	0.722	0.756		0.649	0.71
Cr2O3				*Not(Measured*				
K2O				*Not(Measured*				
CaO	4.771	6.024	4.766	6.731	7.006		7.671	7.04
TiO2				*Not(Measured*				
Total	101.857	101.227	101.19	98.199	98.062		96.66	98.611
				Formula(based(on(12(oxygens(and(8(cations				
Si	3.0372	3.0363	3.0187	3.0563	3.0573		3.0554	3.0668
Mg	0.622	0.5429	0.7551	0.4836	0.479		0.4891	0.453
Na								
Al	1.9236	1.947	1.9632	1.9729	1.9728		1.9858	1.9713
Fe	1.9618	1.8864	1.8152	1.8209	1.7974		1.7146	1.8105
Mn	0.0611	0.076	0.0542	0.0487	0.0511		0.0443	0.0477
Cr								
K								
Ca	0.3952	0.5016	0.3933	0.5748	0.5987		0.6624	0.5984
Ti								
Total	8.0009	7.9903	7.9998	7.9572	7.9563		7.9517	7.9478

Table 1. Continued.

Amphibole	[redacted]	712CE1	[redacted]	H2718D	[redacted]
	Intermediate	Relict/Border	Groundmass	Groundmass	Gm/edge
SiO2	36.267	25.776	43.992	42.143	41.505
MgO	0.053	16.779	12.589	10.776	11.117
Na2O	0	0	2.153	1.755	1.856
Al2O3	28.874	21.628	15.489	15.143	14.827
FeO	5.364	22.891	10.429	12.461	12.682
Fe2O3			*Not(Measured*		
MnO	0.1	0.231	0.08	0.068	0.029
Cr2O3			*Not(Measured*		
K2O	0	0.006	0.289	0.316	0.313
CaO	24.011	0.063	10.964	11.221	11.248
TiO2	0.253	0.019	0.7	0.91	0.919
Total	94.938	87.434	96.708	94.833	94.496
		Formula(based(on(23(oxygens			
Si	5.4014	4.4112	6.3996	6.3319	6.2861
Mg	0.0118	4.2806	2.7299	2.4135	2.5099
Na	0	0	0.6074	0.5113	0.5449
Al	5.0687	4.3628	2.6558	2.6817	2.6469
Fe	0.6681	3.2763	1.2688	1.5658	1.6064
Fe3+					
Mn	0.0127	0.0335	0.0098	0.0086	0.0037
Cr					
Ca	3.8317	0.0116	1.709	1.8065	1.8254
Ti	0.0283	0.0024	0.0766	0.1028	0.1047
Total	15.0362	16.4057	15.5266	15.5104	15.5885

Table 1. Continued.

Plagioclase	[redacted]	712CE1 [redacted]		H2718D [redacted]	
	Core/1	Core/2	Inside/grt	Groundmass	Brittle/Fx
SiO2	67.807	66.534	66.744	67.636	62.965
MgO			*Not(Measured*		
Na2O	11.479	11.349	11.303	11.902	10.001
Al2O3	20.097	20.359	19.649	19.331	21.171
Fe2O3	0.061	0.045	0.082	0	0.529
MnO			*Not(Measured*		
Cr2O3			*Not(Measured*		
K2O	0.014	0.032	0.038	0.012	0.023
CaO	0.91	1.115	0.697	0.392	3.981
TiO2			*Not(Measured*		
Total	100.368	99.434	98.513	99.273	98.67
			Formula(based(on(8(oxygens		
Si	2.9589	2.9353	2.9656	2.9825	2.8309
Mg					
Na	0.9713	0.9709	0.9738	1.0177	0.8719
Al	1.0337	1.0587	1.0291	1.0048	1.1219
Fe+3	0.002	0.0015	0.0027	0	0.0179
Mn					
Cr					
K	0.0008	0.0018	0.0021	0.0007	0.0013
Ca	0.0426	0.0527	0.0332	0.0185	0.1918
Ti					
Total	5.0094	5.0209	5.0066	5.0242	5.0357

analysed so comparison is impossible.

Plagioclase

All of the plagioclase in samples 712C-1 and H2718D is albite. Along fractures in sample H2718D, the albite has higher Al and Ca, but lower Na compared to the standard groundmass albite (Table 1, part 3).

Zr-in-Rutile Geothermometry

Because there is evidence of disequilibrium in the thin sections, the thin sections contain no suitable geothermometers or geobarometers, and there is indication of fluid movement in H2718D and 712C-1, conventional geothermometry cannot be applied to these Catalina garnet-gneiss block samples. Consequently, we used the new Zr-in-rutile thermometer (Spear et al. 2006) for determination of the temperature of metamorphism during garnet growth and for comparison between different blocks and settings.

Using the relation given on p. 17, the zirconium content of rutile equates to metamorphic T's in the vicinity of 500 °C. In sample 712C-1, rutile was analysed as inclusions in different garnet zones and euhedral and anhedral grains in the groundmass (Fig. 12). Rutile grains within garnet have Zr concentrations and temperatures ranging from 27 to 32 ppm and 481 ± 5 °C to 489 ± 4 °C (Table 2). Grains do not show a significant temperature difference between the garnet zones.

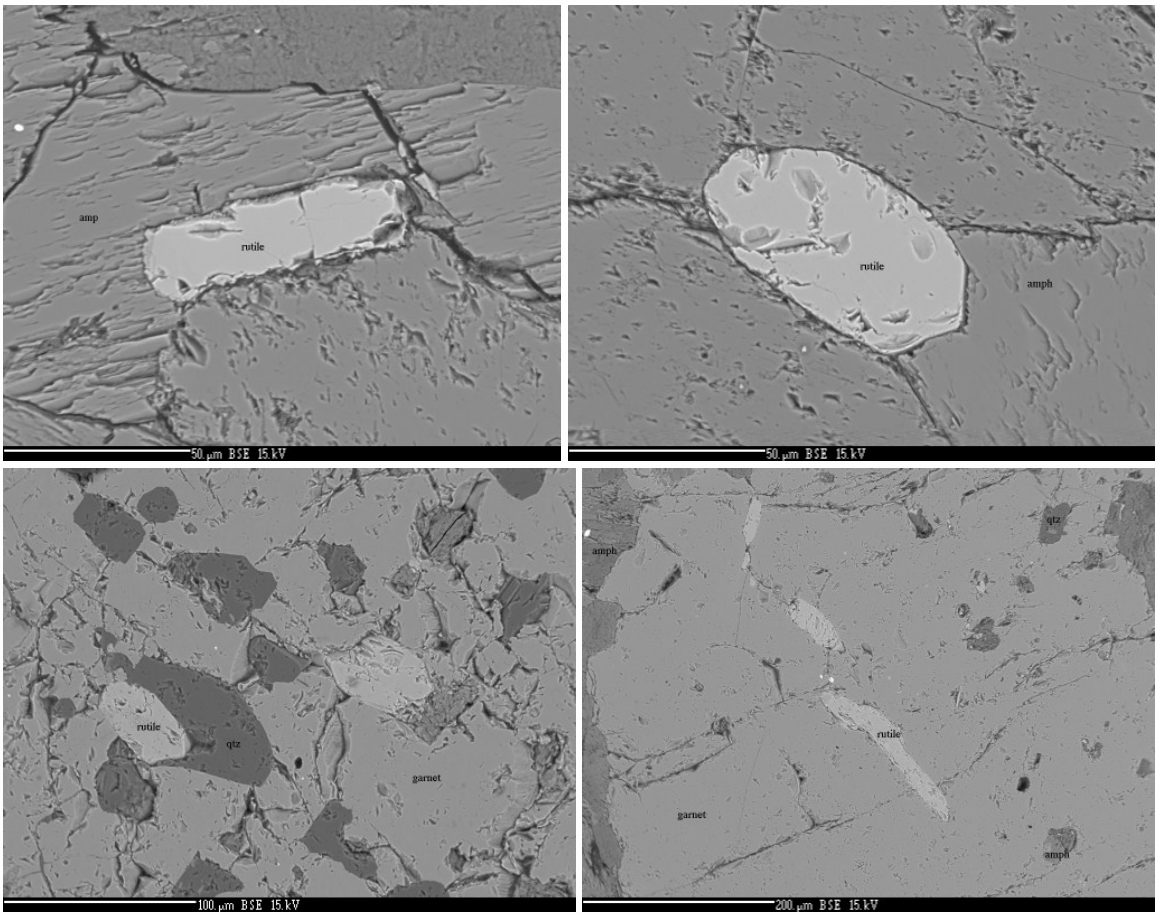

Figure 12. Rutile grains in sample 712C-1 analysed for Zr concentration (ppm). A) Euhedral grain in the groundmass. B) Anhedral grain in the groundmass. C) Rutile inclusions in the intermediate zone. D) Rutile inclusions forming a relict border in garnet. (EMP photos)

Rutile grains within the groundmass have average Zr concentrations and temperature of 40 ppm and 502 ± 3 °C. Euhedral and anhedral rutile grains in the groundmass were analysed and compared, but no difference is discernable.

In sample H2718D rutile inclusions, around the perimeter of garnet, within the brittle fracture, and in the groundmass were analysed (Fig. 13). Many of the large rutile grains have titanite rims, and were found to have lower temperatures, by about 30 °C, compared to rutile lacking titanite rims in the same setting. Because titanite is thought to affect the Zr concentration in rutile (Kapp et al., 2009), rutile

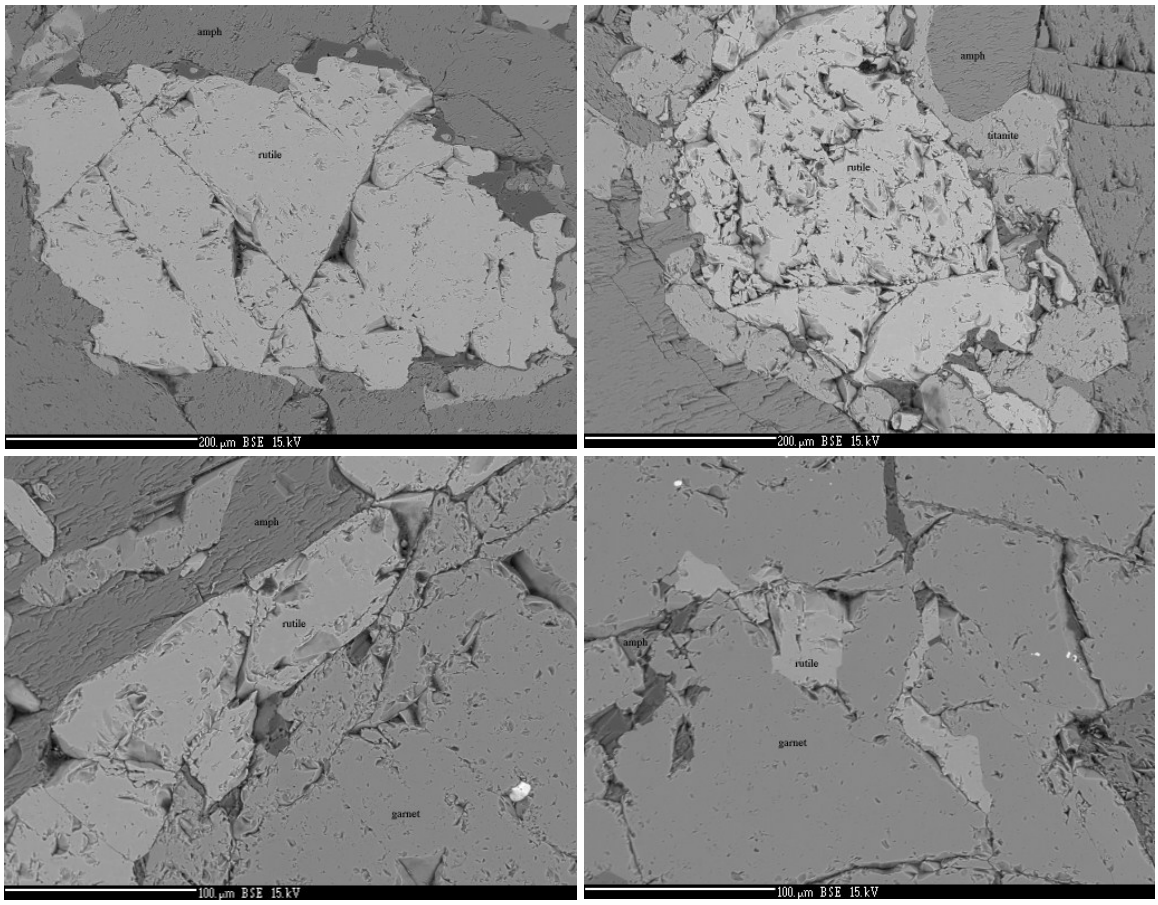

Figure 13. Rutile grains in sample H2718D analysed for Zr concentration (ppm). A) Rutile grain in the groundmass surrounded by amphibole. B) Rutile grain with a titanite rim in the groundmass. C) Rutile grain on the perimeter of garnet. D) Rutile inclusions in garnet. (EMP photos)

Table 2. Zr-in-rutile concentrations and calibrated temperatures.

Sample	Location	No. of spots	Ave Zr ppm	Ave St. Dev.	Ave T (°C)	St. Error
712C-1	Core	10	31.66	6.90	488.83	3.88
	Intermediate	7	30.98	9.68	486.09	7.85
	Relict Border	11	27.69	6.86	480.80	4.68
	Groundmass	15	39.74	6.74	502.23	2.68
H2718D	Inclusions	8	33.34	11.58	489.76	7.85
	Grt Border	2	46.22	1.99	511.85	1.83
	Groundmass	6	49.53	2.24	516.00	1.13
	Brittle Fx	9	33.07	13.04	488.40	8.33

grains with titanite rims were excluded from consideration. Rutile grains within garnet have an average Zr concentration of 33 ppm and temperature of 490 ± 8 °C. Grains that are around the perimeter of garnet have an average Zr concentration of 46 ppm and temperature of 512 ± 2 °C (Table 2). Grains within the groundmass have an average Zr concentration of 50 ppm and temperature of 516 ± 1 °C. Grains within the brittle fracture system have an average Zr concentration of 33 ppm and temperature of 488 ± 8 °C. For all analyses, calculated temperature uncertainties are better than ± 10 °C (Table 2). Therefore, the garnet interior temperatures are lower then those on the perimeter and in the groundmass, demonstrating that garnet grew during increasing metamorphic temperatures. The finding is consistent with the garnet zoning pattern in sample 712C-1, which has an increase in Mg near the rims (Fig. 8C).

DISCUSSION

Samples 712C-1 and H2718D, from separate gneiss blocks within mélange, show differences in their composition and metamorphic history. Sample 712C-1 exhibits changes in major elements and inclusion phases from core to rim in garnet, indicating compositional changes during garnet growth. Mg increasing towards the rim indicates increasing temperature during garnet growth (Sorensen, 1988). The rutile in the groundmass is small, euhedral, and anhedral.

Sample H2718D has compositionally homogenous garnet and no compositional variation in inclusion phases, suggesting that the source block did not

undergo significant compositional change during garnet growth. Rutile formed small inclusions within garnet and immense grains around the perimeter of garnet. Both observations suggest that open system behavior occurred with cations provided from an exterior source, including Titanium for growth of rutile.

In sample H2718D, there is an unusual abundance of rutile, even for a rock having a Ti-basalt protolith. It indicates that (voluminous) fluid moved through the rock, transporting titanium from the serpentinite into the blocks, where it formed rutile. The Zr-in-rutile thermometry study suggest T's of 480 to 516 °C for the event. The absence of rutile between coalesced garnets indicates that the fluid movement occurred after garnet formation.

The results contrast with those of Zack et al. (2004), who analysed Zr-in-rutile for three clinopyroxene bearing garnet amphibolite blocks from Catalina Island (Fig. 14). The temperatures range from 764 to 800 °C, much higher than the temperatures determined from my study. The temperatures obtained in my study suggest that the blocks barely made it into amphibolite grade metamorphic temperatures, whereas the temperatures presented by Zack et al. are on the high end of the amphibolite grade temperatures.

Zr-in-rutile temperatures for rutile inclusions provide minimum temperature for growth of the surrounding garnet (Spear et al., 2006). Zr concentrations in rutile inclusions suggest that garnet growth in sample 712C-1 occurred at T's of 480 to 490 °C. The highest rutile temperatures, of around 502 °C, occur in the groundmass, indicating temperature was increasing during garnet growth.

Conditions for sample H2718D were similar, according to rutile temperatures of ~490 °C within garnet and ~516 °C in the groundmass. The sample records a slight temperature increase during garnet growth

For sample 712C-1, temperature decreased slightly during garnet growth until the relict border, than increased during inclusion free rim growth to the high temperature of the matrix. Sample H2718D only increased in temperature during garnet growth.

There are several potential errors in the Zr-in-rutile analysis. One is that small zircon grains that were in close proximity to the point but not visible could have been excited by the electron beam and increased the measured Zr concentration. Also, partially hitting a hole or pit in the thin section with the electron beam could have caused a lower Zr concentration measurement. It also could be that a pressure correction should be applied, as suggested by Degeling (2002). However, the Watson et al. (2006) calibration uses a suitable pressure of 1.0 GPa, and the pressure that the amphibolite underwent is estimated at 0.8-1.25 GPa, so it is not immediately clear that this would have an effect.

The temperature range established from petrogenetic grid relationships (Fig. 15) is consistent with temperatures obtained for my samples. The presence of garnet and amphibole, albite and epidote replacement textures, the presence of chlorite in sample H2718D, and absence of clinopyroxene indicates that the temperatures should be in a range of 525 to 800 °C (Fig. 15). This is slightly higher than the temperatures determined in this study, but markedly lower than the temperatures found by Zack et al.

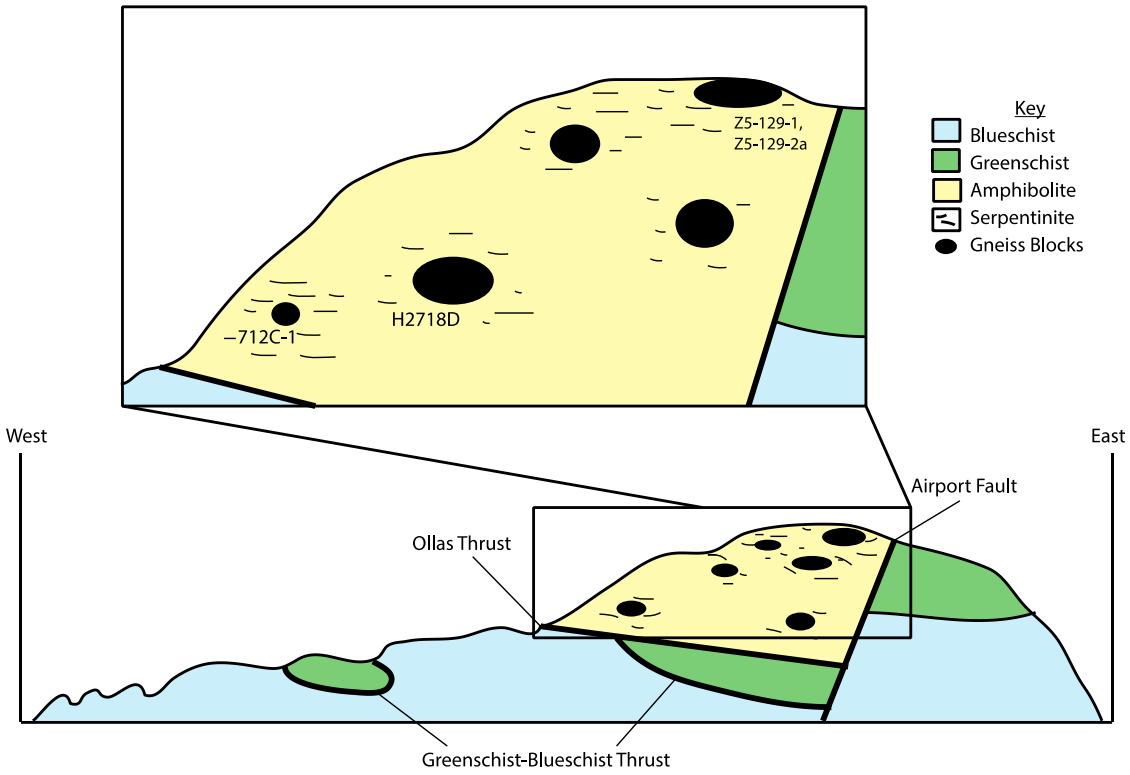

Figure 14. Cross-section of Catalina Island that schematically shows the locations of samples used in this study and by Zack et al. (2004). Not to scale.

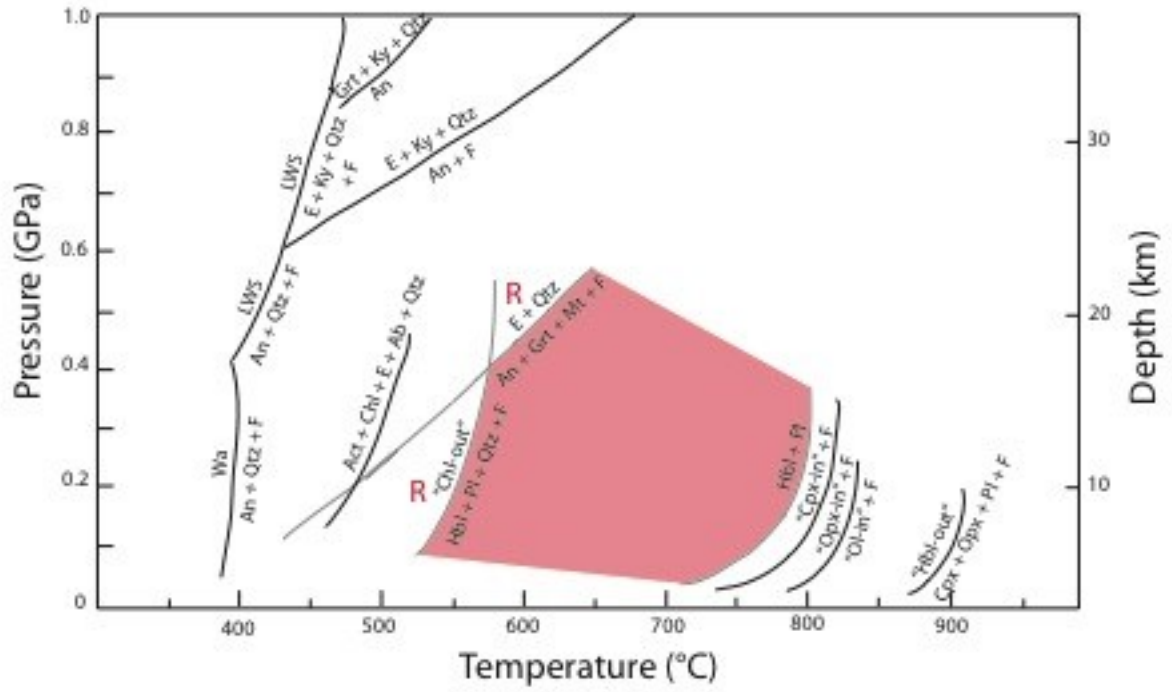

Figure 15. Petrogenetic grid. Red indicates the location of the samples based on the mineralogy. This shows temperatures of 525 to 800 °C for formation of the two samples. The red Rs represent the retrograde minerals. (Based on Winter, 2001)

Assuming rutile formed at P = ~ 1.0-1.5 GPa (Spear et al., 2006) and correlating with measured temperatures of rutile formation, an instantaneous geothermal gradient can be calculated for a point on the rock's P-T path (Spear et al., 2006). Using minimum rutile formation pressure (1.0 GPa) and temperature (480 °C) the geothermal gradient is calculated as ~14 °C/km. This is a relatively low T gradient for a subduction complex. This temperature is for a blueschist more than an amphibolite. This suggests that pressure is needed in order to determine an accurate gradient and location for these blocks.

My findings indicate that the two gneiss blocks studied had distinct protoliths and metamorphic histories, suggesting that mélange blocks within the upper tectonic unit of Catalina Island derived from different locations within a subduction zone. Furthermore, calculated temperatures for metamorphism would have only been sufficient to cause partial melting in the presence of fluids and are lower than previously calculated temperatures determined by previous researchers.

Blocks originating from different depths suggest the possibility of an opportunity to ascertain the conditions and events in different portions of the subduction zone, and therefore significantly further our knowledge and understanding of subduction zones as a whole. However in order for it to be definitively determined if this could be a valid study, a more specific, detailed study of several blocks is necessary to verify whether they do originate in different areas and what information can be ascertained from the blocks.

There are several additional studies that should be done in the future. One is using the titanite-rimmed rutile to obtain an accurate pressure for the H2718D

block (Kapp et al., 2009) that would allow for determination of a more specific depth within the subduction zone. Another is to investigate whether there is temperature-related compositional zoning of the rutile, using Zr-in-rutile. Spear et al. (2006) originally thought that rutile grains did not show zoning. However, very recent unpublished work has suggested that zoning potentially is present in rutile and that this zoning would help to ascertain the progression of movement of the blocks (Spear, pers. comm., 2013).

ACKNOWLEDGEMENTS

I would like to thank Christine Siddoway and F. Zeb Page for their support and help in my research and writing. I gratefully acknowledge Susan Swapp at University of Wyoming and Dan Ruscitto at Rensselaer Polytechnic Institute for assisting me with microprobe analysis. I would also like to thank Steve Weaver for all of his technologic help and instruction. I would like to thank the Keck Geology Consortium and Venture Grant for the funds and opportunity to go to Santa Catalina Island, CA and pursue the use of university instrumentation for the research and analysis for my thesis. I would especially like to thank Emily Walsh, Mitchell Awalt, Mike Barthelmes, Fredy Aguirre, Henry Towbin, and Lauren Magliozzi for their friendship, support, and help on Catalina and throughout the year. I would also like to thank the whole Colorado College Geology Department for nurturing and furthering my love and respect for Geology.

REFERENCES

Baldwin, S.L. and Harrison, T.M., 1992, The P-T-t history of blocks in serpentinite-matrix mélange, west-central Baja California: Geological Society of America Bulletin, v. 104, p. 18-31.

Bebout G.E., and Barton, M.D., 1989, Fluid flow and metasomatism in a subduction zone hydrothermal system: Catalina Schist terrane, California: Geology, v. 17, p. 976-980.

Crawford, M.L., Hollister, L.S., and Woodsworth, G.L., 1987, Crustal deformation and regional metamorphism across a terrane boundary, Coast Plutonic Complex, British Columbia: Tectonics, v. 6, no. 3, p. 343-361.

Degeling, H.S., 2002, Zircon Equilibria in Metamorphic Rocks. Australian National University, Canberra, 460 p.

De Paoli, M.C., Clarke, G.L., and Daczko, N.R., 2012, Mineral equilibria modelling of the granulite-eclogite transition: effects of whole-rock composition on metamorphic facies type-assemblages: Journal of Petrology, v. 35, no. 5, p. 949-970.

Enami, M., Mizukami, T., and Yokoyama, K., 2004., Metamorphic evolution of garnet-bearing ultramafic rocks from Gongen area, Sanbagawa belt, Japan: Journal of Metamorphic Geology, v. 22, p. 1-15.

Encarnación, J.P., Essene, E.J., Mukasa, S.B., and Hall, C.H., 1995, High-pressure and –temperature subohiolitic kyanite-garnet amphibolite generated during initiation of mid-Tertiary subduction, Palawan, Philippines: Journal of Petrology, v. 36, no 6, p. 1481-1503.

García-Casco, A., Torres-Roldán, R.L., Millán, G., Monié, P., and Schneider, J., 2002, Oscillatory zoning in eclogite garnet and amphibole, Northern Serpentinite Melange, Cuba: a record of tectonic instability during subduction?: Journal of Metamorphic Geology, v. 20, p. 581-598.

Grove, M., and Bebout, G.E., 1995, Cretaceous tectonic evolution of coastal southern California: Insights from the Catalina Schist: Tectonics, v. 14, no. 5, p. 1290-1308.

Grove, M., Bebout, G.E., Jacobson, C.E., Barth, A.P., Kimbrough, D.L., King, R.L., Zou, H., Lovera, O.M., Mahoney, B.J., Gehrels, and G.E., 2008, The Catalina Schist: Evidence for middle Cretaceous subduction erosion of southwestern North America, *in* Draut, A.E., Clift, P.D., and Scholl, D.W., eds., Formation and

Applications of the Sedimentary Record in Arc Collision Zones: Geological Society of America Special Paper 436, p.335-361.

Jacobson, C.E., Grove, M., Pedrick, J.N., Barth, A.P., Marsaglia, K.M., Gehrels, G.E., and Nourse, J.A., 2011, Late Cretaceous-early Cenozoic tectonic evolution of the southern California margin inferred from provenance of trench and forearc sediments: Geologic Society of America Bulletin, v. 123, no. 3-4, p. 485-506.

Kapp, P., Manning, E., and Tropper, P., 2009, Phase-equilibrium constraints on titanite and rutile activities in mafic epidote amphibolites and geobarometry using titanite-rutile equilibria: Journal of Metamorphic Geology, v. 27, p. 509-521.

Platt, J.P., 1975, Metamorphic and deformational processes in the Franciscan Complex, California: Some insights from the Catalina Schist terrane: Geological Society of America Bulletin, v. 86, p. 1337-1347.

Powell, R. and Holland, T.J.B., 2008, On Thermobarometry: Journal of Metamorphic Geology, v. 26, p. 155-179.

Powell, R., Holland, T., and Worley, B, 1998, Calculating phase diagrams involving solid solutions via non-linear equations, with examples using THERMOCALC: Journal of Metamorphic Geology, v. 16, p. 577-588.

Sorensen, S.S., 1988, Petrology of amphibolite-facies mafic and ultramafic rocks from the Catalina Schist, southern California: metasomatism and migmatization in the subduction zone metamorphic setting: Journal of Metamorphic Geology, v. 6, p. 405-435.

Sorensen, S.S., and Barton, M.D., 1987, Metasomatism and partial melting in a subduction complex Catalina Schist, southern California: Geology, v. 15, p. 115-118.

Sorensen S.S., and Grossman, J.N., 1989, Enrichment of trace elements in garnet amphibolites from a paleo-subduction zone: Catalina Schist, southern California: Geochimica et Cosmochimica Acta, v. 53, p. 3155-3177.

Spear, F.S., 1993, Metamorphic Phase Equilibria and Pressure-Temperature-Time Paths: Washington, D.C., Mineralogical Society of America, p. 516-545.

Spear, F.S., Wark, D.A., Cheney, J.T., Schumacher, J.C., and Watson, E.B., 2004, Zr-in-rutile thermometry in blueschists from Sifnos, Greece: Contributions to Mineralogy and Petrology, v. 152, p. 375-385.

Wakabayashi, J., 1990, Counterclockwise P-T-t paths from amphibolites, Franciscan Complex, California: relics from the early stages of subduction zone metamorphism: The Journal of Geology, v. 98, no. 5, p. 657-680.

Watson, E.B., Wark, D.A., and Thomas, J.B, 2006, Crystallization thermometers for zircon and rutile: Contributions to Mineralogy and Petrology, v. 151, p. 413-433.

White, R.W., and Powell, R., 2002, Melt loss and the preservation of granulite facies mineral assemblages: Journal of Metamorphic Geology, v. 20, p. 621-632.

Whitney, D., 2013, "Classical" Thermobarometry, The Science Education Research Center at Carleton College: http://serc.carleton.edu/research_education/equilibria/classicalthermobarometry.html (accessed January 2013)

Worley, B., and Powell, R., 2000, High-precision relative thermobarometry: theory and a worked example: Journal of Metamorphic Geology, v. 18, p. 91-101.

Zack, T., Moraes, R., and Kronz, A., 2004, Temperature dependence of Zr in rutile: empirical calibration of a rutile thermometer: Contributions to Mineralogy and Petrology, v. 148, p. 471-488.